

Extract Euler Angles from the General Rotation Transformation Matrix

(http://www.jwave.vt.edu/~rkriz/Projects/Sij_glyphs/npib_Sij_glyphs/Estab_or/Aij-to-Eulerangles.doc)

R.D. Kriz (07-23-06)

Problem Description: Visually represent the state of principal stress for any arbitrary second order stress tensor, σ_{ij} , by drawing three-dimensional (3D) eigen-value shapes and their corresponding eigen-vector orientations. Four possible eigen-value shapes are shown here: 1) quadric [1], 2) HWY [2], 3) Reynolds [3], and 4) PNS [4]. Here we focus on orientations (eigen-vectors) of these shapes by using a sequence of three Euler angle rotations. This technique is used to calculate and display the principal stress state for residual stress shown in Fig. 2. Euler angles are typically required to draw these orientations using graphical packages such as VRML-1 or -2 as well as PV-Wave. Hence many graphics computer programmers prefer to work with Euler angle rotations. However most scientific subroutine packages (e.g. IMSL, NAG, etc.) return a 3x3 transformation matrix, a_{ij} , where each column corresponds to an eigen-vector orientation unique to each eigen-value. This same matrix, a_{ij} , is also defined by Frederick and Chang, pp. 6-11, Ref. [1], and used to transform rectangular Cartesian coordinates, X_j , as a first order tensors $X_i' = a_{ij} X_j$. Hence our task is to calculate the Euler angles from this a_{ij} transformation matrix.

Objective: Given: a_{ij} , **Find:** Euler angles ($\theta_x, \theta_y, \theta_z$). This is accomplished by creating a transformation matrix, a_{ij} , from a sequence of three simple rotations in Fig. 1. Because the rotation matrix, a_{ij} , is constructed from Euler angle rotations, these angles can be extracted from this matrix using simple algebra. Here we use the same procedure and notation outlined by Bourke [5]. The coordinate system shown in Fig. 1 is typically used in flight simulators with the origin located at the aircraft centroid, with the y-axis pointing forward, the x-axis off the right wing and the z-axis pointing up. This is the same convention is used by the DIVERSE API [6]. Rotation sequence is as follows: (1) “roll” positive to the right, (2) “pitch” positive up, and (3) “yaw” positive to the left. Note: order matters, (1) \rightarrow (2) \rightarrow (3) is not equal to (2) \rightarrow (1) \rightarrow (3).

(1) “roll” right, $+\theta_y$

$$\begin{bmatrix} X' \\ Y' \\ Z' \end{bmatrix} = \begin{bmatrix} \cos(\theta_y) & 0 & -\sin(\theta_y) \\ 0 & 1 & 0 \\ \sin(\theta_y) & 0 & \cos(\theta_y) \end{bmatrix} \begin{bmatrix} X \\ Y \\ Z \end{bmatrix} \quad (1)$$

(2) “pitch” up, $+\theta_x$,

$$\begin{bmatrix} X' \\ Y' \\ Z' \end{bmatrix} = \begin{bmatrix} 1 & 0 & 0 \\ 0 & \cos(\theta_x) & \sin(\theta_x) \\ 0 & -\sin(\theta_x) & \cos(\theta_x) \end{bmatrix} \begin{bmatrix} X \\ Y \\ Z \end{bmatrix} \quad (2)$$

(3) “yaw” left, $+\theta_z$,

$$\begin{bmatrix} X'' \\ Y'' \\ Z'' \end{bmatrix} = \begin{bmatrix} \cos(\theta_z) & \sin(\theta_z) & 0 \\ -\sin(\theta_z) & \cos(\theta_z) & 0 \\ 0 & 0 & 1 \end{bmatrix} \begin{bmatrix} X' \\ Y' \\ Z' \end{bmatrix} \quad (3)$$

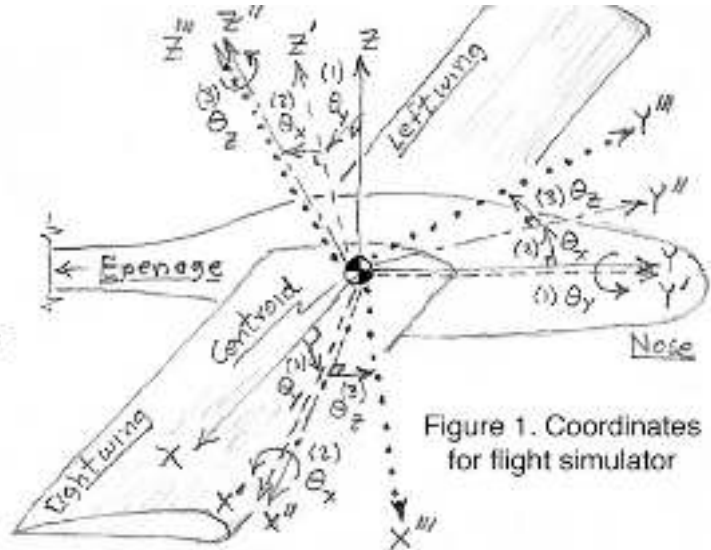


Figure 1. Coordinates for flight simulator

For brevity the following notation is used, for cosines: $ctx = \cos(\theta_x)$, $cty = \cos(\theta_y)$, $ctz = \cos(\theta_z)$, and for sines: $stx = \sin(\theta_x)$, $sty = \sin(\theta_y)$, $stz = \sin(\theta_z)$. Combine roll followed by pitch.

$$\begin{bmatrix} cty & 0 & -sty \\ (stx)(sty) & ctx & (stx)(cty) \\ (ctx)(sty) & -stx & (ctx)(cty) \end{bmatrix} \begin{bmatrix} 1 & 0 & 0 \\ 0 & ctx & stx \\ 0 & -stx & ctx \end{bmatrix} \begin{bmatrix} cty & 0 & -sty \\ 0 & 1 & 0 \\ sty & 0 & cty \end{bmatrix} \begin{bmatrix} X' \\ Y' \\ Z' \end{bmatrix} = \begin{bmatrix} X'' \\ Y'' \\ Z'' \end{bmatrix} \quad (4), \quad \begin{bmatrix} X' \\ Y' \\ Z' \end{bmatrix} = \begin{bmatrix} cty & 0 & -sty \\ (stx)(sty) & ctx & (stx)(cty) \\ (ctx)(sty) & -stx & (ctx)(cty) \end{bmatrix} \begin{bmatrix} X \\ Y \\ Z \end{bmatrix} \quad (5)$$

Combine the roll and pitch transformation (4) above with the yaw transformation (3).

$$\begin{bmatrix} (ctz)(cty)+(stz)(stx)(sty) & (stz)(ctx) & -(ctz)(sty)+(stz)(stx)(cty) \\ -(stz)(cty)+(ctz)(stx)(sty) & (ctz)(ctx) & (stz)(stz)+(ctz)(stx)(cty) \\ (ctx)(sty) & -stx & (ctx)(cty) \end{bmatrix} = \begin{bmatrix} ctz & stz & 0 \\ -stz & ctz & 0 \\ 0 & 0 & 1 \end{bmatrix} \begin{bmatrix} ctx & 0 & -stz \\ (stx)(sty) & ctx & (stx)(cty) \\ (ctx)(sty) & -stx & (ctx)(cty) \end{bmatrix} \quad (6)$$

Combining all three transformations (1) -> (2) -> (3) yields the final transformation $X_i''' = a_{ij} X_j$, where $a_{11} = (ctz)(cty) + (stz)(stx)(sty)$, $a_{12} = (stz)(ctx)$, $a_{13} = -(ctz)(sty) + (stz)(stx)(cty)$, etc..

$$\begin{bmatrix} X'' \\ Y'' \\ Z'' \end{bmatrix} = \begin{bmatrix} (ctz)(cty)+(stz)(stx)(sty) & (stz)(ctx) & -(ctz)(sty)+(stz)(stx)(cty) \\ -(stz)(cty)+(ctz)(stx)(sty) & (ctz)(ctx) & (stz)(stz)+(ctz)(stx)(cty) \\ (ctx)(sty) & -stx & (ctx)(cty) \end{bmatrix} \begin{bmatrix} X \\ Y \\ Z \end{bmatrix} \quad (7)$$

Recall notation $-stx = -\sin(\theta_x) = +a_{32}$ and collecting terms a_{31}/a_{33} and a_{12}/a_{22} , reduces terms to $a_{31}/a_{33} = [\cos(\theta_x) \sin(\theta_y)] / [\cos(\theta_x) \cos(\theta_y)] = \tan(\theta_y)$, and $a_{12}/a_{22} = \tan(\theta_z)$, and yields Euler angles,

$$\theta_x = \sin^{-1}(-a_{32}), \theta_y = \tan^{-1}(a_{31}/a_{33}), \text{ and } \theta_z = \tan^{-1}(a_{12}/a_{22}).$$

These Euler angles are used to orient quadric, Reynolds, HWY, and PNS stress tensor glyphs using VRML-1 and -2 syntax [7], shown below in Fig. 2. These file formats can be viewed using popular web-browser plugins and also in immersive virtual environments.

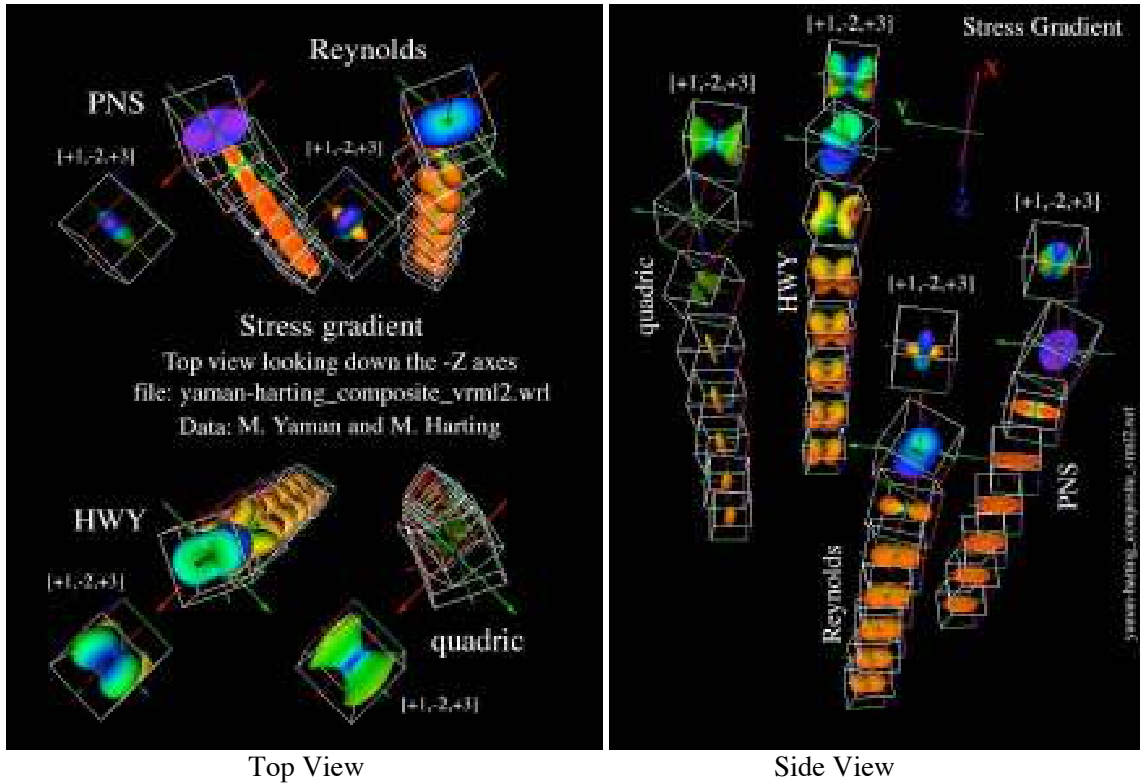


Figure 2. Residual principal stress gradients for shot peened Ti-6AL-4V, Stress glyph gradient development, Kriz, Yaman, and Harting [7], Data: Harting [8]

Rotational gradients of principal stress states (eigen-vectors) are best observed in the Top View of Fig. 2. However this view obscures gradients of eigen-value shapes. Gradients in eigen-value shapes are best observed in the Side View. Principal stress state glyphs at [+1,-2,+3] are shown for each glyph type, which provides a comparative reference. These gradients are best observed in an immersive virtual environment where the observer can literally walk into this 3D space and view the gradients from any arbitrary angle for enhanced analysis and interpretation.

References:

1. Frederick, D. and Chang, T.S., Continuum Mechanics, Scientific Publishers, Inc. Boston. pp. 38-40, 1972.
2. Hashash, Y.M.A. Yao, J.I., and Worting, D.C., "Glyph and hyperstream representation of stress and strain tensors and material constitutive response, Int. J. Numer. and Anal. Meth. in Geomech., Vol 27, pp 603-626, 2003.
3. Moore, J.G., Schorn, S.A., and Moore, J., "Methods of Classical Mechanics Applied to Turbulence Stresses in a Tip Leakage Vortex, Conference Proceedings of the ASME Gas Turbine Conference, Houston, Texas, October, 1994, (also Turbomachinery Research Group Report No. JM/94-90).
4. Kriz, R.D., Yaman, M., Harting, M., and Ray A.A., "Visualization of Zeroth, Second, Fourth, Higher Order Tensors, and Invariance of Tensor Equations, submitted for publication, 2006. Contact rkriz@vt.edu for a draft of this paper.
5. P. Bourke, Euler Angles: <http://local.wasp.uwa.edu.au/~pbourke/projection/eulerangle/>
6. DIVERSE virtual environment API: <http://diverse.sourceforge.net>
7. Kriz, R.D., Yaman, M., and Harting, M., "Residual Stress Gradient Visualization" http://www.sv.vt.edu/future/vt-cave/VT/residual-stress/residual_stress.html, "Syntax for VRML-1 and -2 used to establish glyph orientation": http://www.jwave.vt.edu/~rkriz/Projects/Sij_glyphs/npib_Sij_glyphs/Estab_or/, "FORTRAN program calculates eigenvalues, -vectors and Euler angles from second order stress tensors": http://www.jwave.vt.edu/~rkriz/Projects/Sij_glyphs/npib_Sij_glyphs/TP/surf121/eigen.f,
8. Harting, M., "A semi-numerical method to determine the depth profile of the three dimensional residual stress state with x-ray diffraction", Acta Mater, Elsevier Science, Vol. 46, no. 4, pp. 1427-1436, 1998.